A New Method for Dielectric Characterization in Sub-THz Frequency Range

Yevhen Yashchyshyn, *Senior Member, IEEE*, and Konrad Godziszewski, *Member, IEEE*

***Abstract*—A new method for broadband characterization of dielectrics in the sub-terahertz (sub-THz) frequency range is presented. Quasi-optical free space measurement setup is used to determine the complex reflection coefficient in a wide frequency band. This method makes it possible to characterize every dielectric by using only the measured complex reflection coefficient without accurate information about the thickness of dielectric sample. This method is useful in case of lossy and/or thick dielectric samples and is based on modern measurement equipment feasibility, with the possibility to make measurements in high number of frequency points. The mathematical model of the method is formulated. Finally, results of measurements for different dielectrics are presented. The obtained permittivity values of these dielectrics are comparable to those reported in the literature.**

***Index Terms*—Permittivity, standing wave ratio (SWR), sub-terahertz (sub-THz) measurements.**

I. Introduction

MATERIAL characterization in the sub-terahertz (sub-THz) frequency range is becoming increasingly important due to a large number of applications in this band. This is due in part to the broad availability of this band and specific propagation characteristics in different media. The most common applications are radars, high data rate communication systems, spectroscopy or security scanners. Therefore, to appropriately model electromagnetic properties of devices for such applications, it is necessary to first determine properties of materials. In particular, the value of the complex permittivity is important. Precise determination of the value of this parameter is strictly required for both designers and manufacturers of electronic systems. Hence, there is a great interest in these types of measurements and research activities continue to improve existing measurement techniques or to develop new ones.

Over the years different methods for obtaining the permittivity and permeability of a given material have been developed [1], [2]. Measurement methods include open-ended and closed-ended transmission line techniques, cavity and dielectric resonator techniques, transmission-line techniques, near-field scanning probes, and free-space techniques.

Open and closed-ended transmission lines can be used to obtain permittivity in very wide frequency range using relatively simple instrumentation. This approach is very simple and does not require any complicated measurement equipment, although it has some drawbacks and limitations. First, physical realization of this concept in a sub-THz waveguide is practically impossible due to the small dimensions of the transmission line. For this reason, it is also very difficult to prepare an appropriate sample to test. Additionally, air gaps between specimens and the end of the line are difficult to avoid with hard solid specimens.

Resonators and cavities are a special class of measurement cells that are especially useful for measuring very low loss materials [3]–[5]. They also offer the highest accuracy of measurement of real permittivity, but only in one or a few frequency points. These methods have limited measurement capabilities at higher frequencies, mainly due to decreasing precision of fabrication.

Some of the most suitable methods for measurement in the sub-THz range are free space quasi-optical techniques. One example of such a method for narrow-band measurements is described in [6]. The approach is based on the Mach-Zehnder interferometer and involves considerable complexity of the measurement system, problems with appropriate arrangement of its particular components, and the need of precise movement of its elements. The last aspect is very important, if measurements are performed in the range of very high frequencies. Short wavelengths necessitate the use of highly accurate, and at the same time expensive, mechanical elements. There are also many other free space methods, which are based on scattering matrix measurements [7]–[9].

THz time-domain spectroscopy (THz-TDS) is commonly used for wide-band characterization [10]. However, its usefulness is limited due to the low power spectral density of the excitation signal and limited SNR in the lower frequency range (below 300 GHz).

Taking into account all aforementioned limitations, we developed a new frequency-domain measurement technique based on the standing-wave concept. The presented method utilizes capabilities of a modern measurement equipment setup [11] based on the vector network analyzer (VNA) with a set of frequency extenders, which enable measurement of scattering parameters in a very wide frequency band (up to 500 GHz in our case). The presented method only requires the complex reflection coefficient for permittivity characterization. It opens up new measurement

Manuscript received April 6, 2017; revised July 3, 2017 and October 23, 2017; accepted October 27, 2017. Date of publication December 4, 2017; date of current version January 9, 2018. This work was supported in part by The National Center for Research and Development (NCBiR), Poland, under Contract PBS3/A3/18/2015. *(Corresponding author: Konrad Godziszewski.)*

The authors are with the Institute of Radioelectronics and Multimedia Technology, Warsaw University of Technology, Warsaw 00-665, Poland (e-mail: E.Jaszczyszyn@ire.pw.edu.pl; K.Godziszewski@ire.pw.edu.pl).

Color versions of one or more of the figures in this paper are available online at http://ieeexplore.ieee.org.

Digital Object Identifier 10.1109/TTHZ.2017.2771309

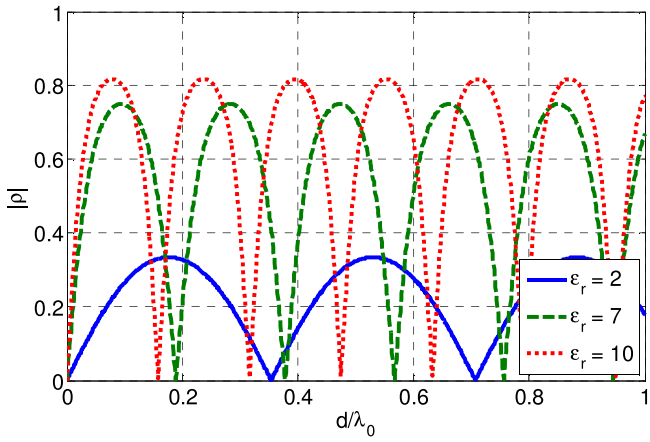

Fig. 1. Example of reflection coefficient for variable thickness of the dielectric layer and different permittivity.

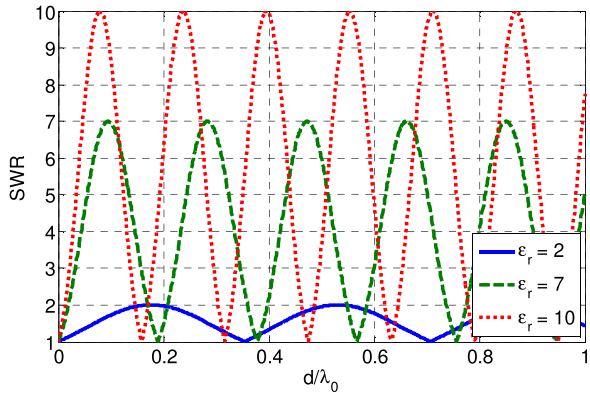

Fig. 2. Example of SWR distribution for variable thickness of the dielectric layer and different permittivity.

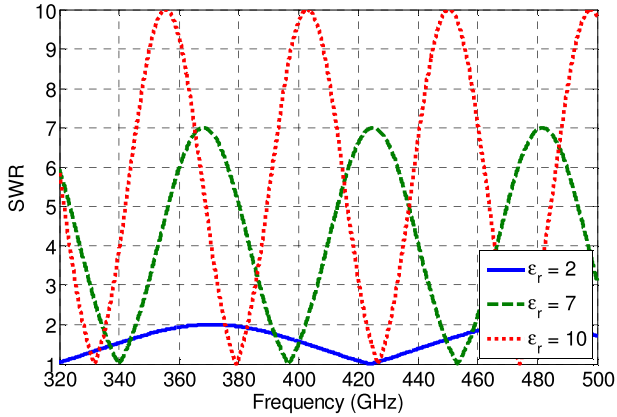

Fig. 3. Example of SWR distribution in the frequency domain for different permittivity.

possibilities that lead to simplified dielectric characterization and, what is even more important, allows remote characterization, because it does not need accurate thickness of the dielectric sample.

II. Theoretical Study

A. Lossless Dielectrics

Let us consider two isotropic half-spaces of the same relative permittivity ε_{r1} equals to 1 separated by lossless isotropic dielectric flat layer of relative permittivity ε_{r2} and thickness d. Plane wave $E(t,x) = E_0 \exp(j\omega_0 t - jkx)$, (where $k = 2\pi/\lambda_0$, λ_0 is the wavelength of the incident wave, $\omega_0 = 2\pi f_0 = 2\pi c/\lambda_0$, c is the speed of light) is perpendicularly incident upon the dielectric layer boundary from, for example, the left half-space. If we assume that the dielectric is lossless, it is obvious that the field distribution in the space between source and dielectric layer (along the x-axis) depends on permittivity and thickness of this layer.

If the thickness of the dielectric layer is a multiple of half of the wavelength in this medium $\lambda_2 = \lambda_0/\sqrt{\varepsilon_{r2}}$, the dielectric layer becomes transparent. This means that no reflection is observed in the first half-space. The opposite situation occurs for an odd multiple of quarter wavelength thickness where maximum reflection takes place. Fig. 1 shows the magnitude of the reflection coefficient depending on thickness of layer d for different permittivity: $\varepsilon_{r2} = 2;\ 7;\ 10$.

If we introduce a new parameter, which is similar to conventional definition of the standing wave ratio (SWR), but dependent on thickness of the dielectric layer, then maximum $\mathrm{SWR}(d)$ is directly equal to the permittivity of layer (see Fig. 2)

$$\mathrm{SWR}(d)_{\max} = \frac{1 + |\rho(d)|_{\max}}{1 - |\rho(d)|_{\max}} = \varepsilon_{r2} \tag{1}$$

where ρ is the complex reflection coefficient referenced to the layer boundary from which the reflection is measured.

It can be clearly seen that the maximum of $\mathrm{SWR}(d)$ distribution is equal to the relative permittivity of the dielectric layer which is equal to 2, 7, and 10, respectively. This observation allows for fast determination of permittivity of the given dielectric without solving complicated mathematical equations. However, the practical implementation of this concept is very difficult due to the need to produce many samples of accurately known thickness. This is because maximum $\mathrm{SWR}(d)$ can only be found for a given specific thickness of the layer. To overcome these difficulties, we propose to substitute it for wide-band reflection coefficient measurement and calculation of SWR distribution in the frequency domain. This idea is new, and it constitutes the main subject of the paper.

When reflection coefficient is measured in the frequency domain, analogous equation for maximum $\mathrm{SWR}(f)$ can be written as follows:

$$\mathrm{SWR}(f)_{\max} = \frac{1 + |\rho(f)|_{\max}}{1 - |\rho(f)|_{\max}} = \varepsilon_{r2}. \tag{2}$$

Fig. 3 presents $\mathrm{SWR}(f)$ calculated assuming the same permittivity values as previously and thickness $d = 1$ mm.

Similarly to the previous situation, for certain frequencies the maximum value of $\mathrm{SWR}(f)$ equals the relative permittivity. However, to be able to use this principle, the sample under test has to be appropriately thick. Electrical thickness of the

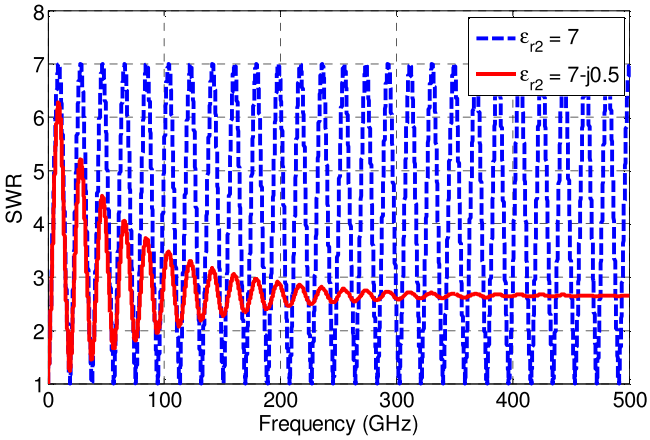

Fig. 4. Example of SWR distribution for lossless and lossy sample.

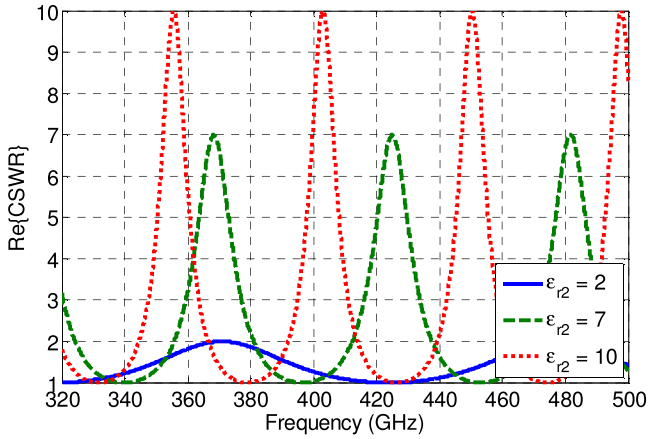

Fig. 5. Real part of CSWR for different lossless samples.

sample determines the number of $\mathrm{SWR}(f)$ maxima in the given frequency range Δf

$$n = \left\lceil \frac{2d\sqrt{\varepsilon_{r2}}\Delta f}{c} \right\rceil. \tag{3}$$

It should be also mentioned that a large number of maxima makes determining the permittivity for greater number of frequency points possible. It is very important in the case of dispersive dielectrics whose parameters are not constant in a broad frequency range. Nevertheless, requirement of thick samples is a significant advantage of this method because many other methods require relatively thin samples to achieve good results. Additionally, in this approach, the thickness of the sample need not be known, because this parameter is not used for permittivity calculations. Moreover, in many other measurement methods, thickness uncertainty is the most significant component of measurement uncertainty [12].

B. Lossy Dielectrics

In case of lossy dielectrics, a similar relation between $\mathrm{SWR}(f)$ distribution and complex permittivity $\varepsilon_{r2} = \varepsilon_{r2}{}' - j\varepsilon_{r2}{}'' = \varepsilon_{r2}{}'(1 - j\tan\delta_2)$ also exists. However, for lossy dielectrics, the local maxima of $\mathrm{SWR}(f)$ distribution are related to real and imaginary parts of permittivity. In Fig. 4, a comparison between SWR distribution for lossless and lossy dielectric is presented. Calculations were made for a 3-mm-thick sample of $\varepsilon_{r2} = 7$ and $\varepsilon_{r2} = 7 - \mathrm{j}0.5$, respectively.

It is not possible to obtain properties of a lossy dielectric based on the presented approach (2) because $SWR(f)$ does not contain enough information. For this reason, we propose to introduce a new parameter—complex SWR (CSWR)—defined as

$$\mathrm{CSWR}\,(f) \overset{\mathrm{def.}}{=} \frac{1-\rho\,(f)}{1+\rho\,(f)}. \tag{4}$$

For lossless samples, only the real part of $\mathrm{CSWR}(f)$ is needed to obtain the permittivity, and it can be proved that in this case, there is an equation equivalent to (2)

$$\mathrm{Re}\{\mathrm{CSWR}\,(f)\}_{\max} = \varepsilon_{r2}. \tag{5}$$

In Fig. 5, the real part of $\mathrm{CSWR}(f)$ for different lossless samples is presented. The maxima of each plot are equal to particular permittivity values, the same as in Fig. 3.

For the opposite situation of very high losses, the real part of $\mathrm{CSWR}(f)$ tends to be constant in the given frequency range. It can be seen in Fig. 4 (red line) around 500 GHz. High losses cause there to be no reflection from the opposite boundary of the dielectric layer, a scenario similar to the reflection from the boundary between two half-spaces with different relative permittivity.

In this case, $\mathrm{CSWR}(f)$ is given as follows:

$$\mathrm{CSWR}\,(f) = \sqrt{\varepsilon_{r2}} \tag{6}$$

and its real part and phase are given by

$$\mathrm{Re}\,\{\mathrm{CSWR}\,(f)\} = \sqrt{\varepsilon_{r2}{}'} \cdot \sqrt{\frac{1+\sqrt{1+\tan^2\delta_2}}{2}} \tag{7}$$

$$\arg\{\mathrm{CSWR}\,(f)\} = \arctan\left(-\sqrt{\frac{\sqrt{1+\tan^2\delta_2}-1}{\sqrt{1+\tan^2\delta_2}+1}}\right). \tag{8}$$

Solving the foregoing equations, the real part of permittivity and loss tangent can be determined

$$\varepsilon_{r2}{}' = \frac{2[\mathrm{Re}\,\{\mathrm{CSWR}\,(f)\}]^2}{1+\sqrt{1+\tan^2\delta_2}} \tag{9}$$

$$\tan\delta_2 = \frac{2\tan\left[\arg\{\mathrm{CSWR}\,(f)\}\right]}{\tan^2\left[\arg\{\mathrm{CSWR}\,(f)\}\right]-1}. \tag{10}$$

The most interesting fact is that: in case of high losses the phase of $\mathrm{CSWR}(f)$ only depends on the loss tangent. Furthermore, the thickness of the sample need not be known to obtain dielectric properties. It seems that it is easier to measure the phase of $\mathrm{CSWR}(f)$ and determine dielectric losses than in the case of the conventional approach. For example, if the phase of

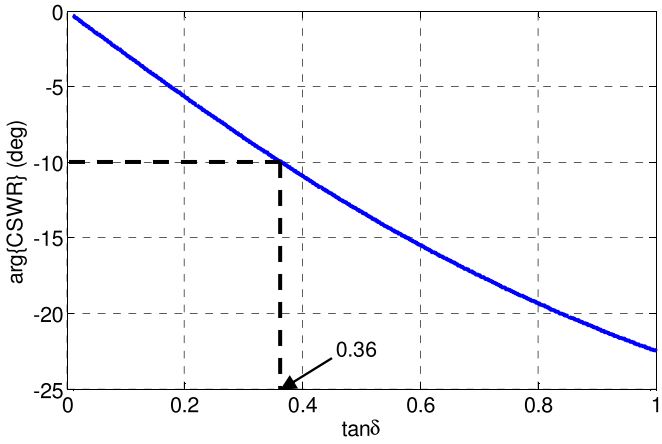

Fig. 6. Phase of CSWR versus loss tangent.

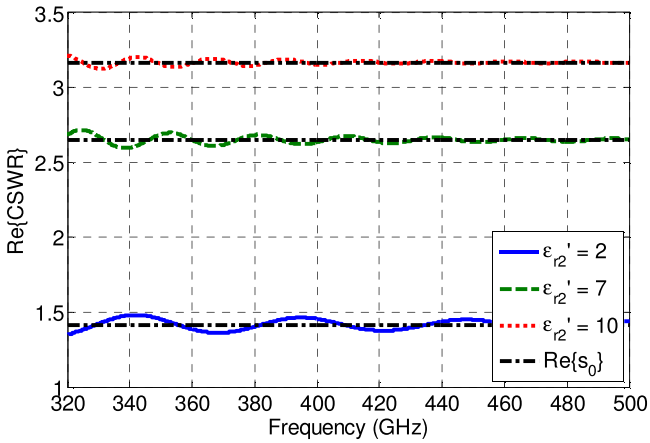

Fig. 7. Real part of CSWR for different lossy samples.

$\mathrm{CSWR}(f)$ is equal to $-10°$, it means that the loss tangent is around 0.36 (as illustrated in Fig. 6).

If the following condition is met, the amplitude of CSWR ripples is less than desired level (ξ):

$$\tan\delta_2 > \frac{\ln(\xi)\,\lambda_0\sqrt{4\pi^2\varepsilon_{r2}{}'d^2 + \ln^2(\xi)\,\lambda_0{}^2}}{2\pi^2 d^2 \varepsilon_{r2}{}'}. \tag{11}$$

When we deal with a sample made of lossy dielectric and assumption (11) is not satisfied, the maxima of the real part and the phase of $\mathrm{CSWR}(f)$ decay with frequency, as presented in Figs. 7 and 8, respectively. Plots were obtained assuming $\tan\delta_2 = 0.1$ and $d = 2$ mm.

For this reason, relation (5) is not valid for such samples, however dielectric properties can also be found by measuring CSWR. For every dielectric (lossless and lossy) one can calculate the Inverse Fourier transform of $\mathrm{CSWR}(f)$. In this way, complex permittivity is related to the zero frequency component of the transform. The real part of zero component (s_0) is

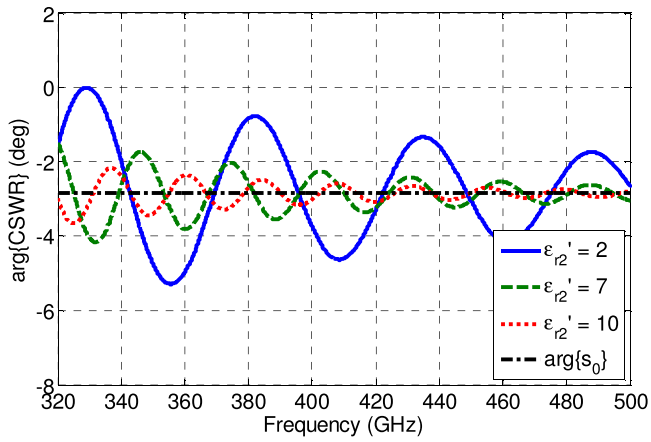

Fig. 8. Phase of CSWR for different lossy samples.

equal to

$$\begin{aligned}\mathrm{Re}\{s_0\} &= \frac{1}{f_2 - f_1}\int_{f_1}^{f_2}\mathrm{Re}\{\mathrm{CSWR}(f)\}df \\ &= \sqrt{\varepsilon_{r2}{}'}\cdot\sqrt{\frac{1+\sqrt{1+\tan^2\delta_2}}{2}}\end{aligned} \tag{12}$$

and its phase is given by

$$\begin{aligned}\arg\{s_0\} &= \arctan\left(\frac{\mathrm{Im}\{s_0\}}{\mathrm{Re}\{s_0\}}\right) \\ &= \arctan\left(-\sqrt{\frac{\sqrt{1+\tan^2\delta_2}-1}{\sqrt{1+\tan^2\delta_2}+1}}\right).\end{aligned} \tag{13}$$

These equations are true when the integration bandwidth includes multiple CSWR periods or sufficient number of ripples. The permittivity and loss tangent can be calculated as

$$\varepsilon_{r2}{}' = \frac{2(\mathrm{Re}\{s_0\})^2}{1+\sqrt{1+\tan^2\delta_2}} \tag{14}$$

$$\tan\delta_2 = \frac{2\tan(\arg\{s_0\})}{\tan^2(\arg\{s_0\})-1}. \tag{15}$$

In Figs. 7 and 8, the corresponding values of real part $\mathrm{Re}\{s_0\}$ and phase $\arg\{s_0\}$ of zero component s_0 are plotted.

Summarizing, it is possible to directly visualize the result of dielectric characterization using the proposed measurement method and modern VNA with Fourier transform option.

III. Measurement Setup and Uncertainty Analysis

Quasi-optical measurement setup used in this study was based on the VNA [14] with frequency extenders [15], enabling complex reflection coefficient measurement from 10 MHz to 500 GHz (up to 32 001 frequency points). The setup is presented in Fig. 9.

It is very important to ensure appropriate measurement conditions—good alignment of all elements of the setup and plane or quasi-plane wave excitation. These conditions can be

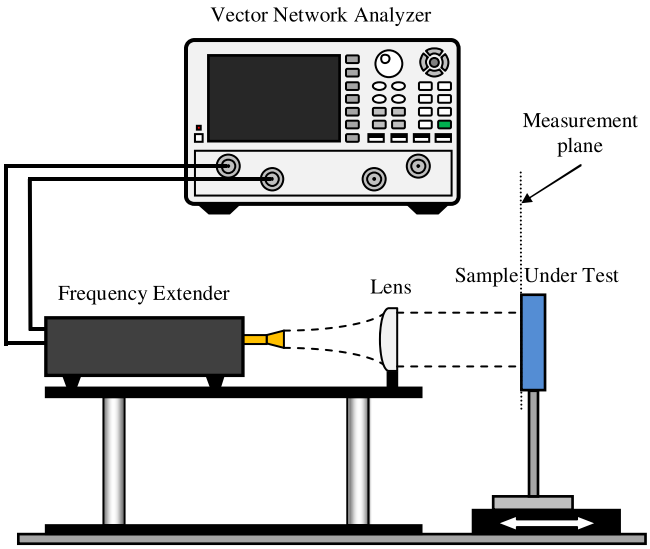

Fig. 9. Scheme of the measurement setup.

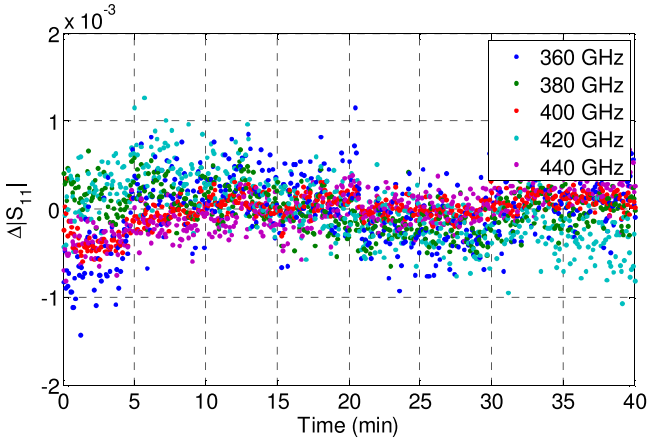

Fig. 10. Stability of the measured magnitude of S_{11} for a few frequencies.

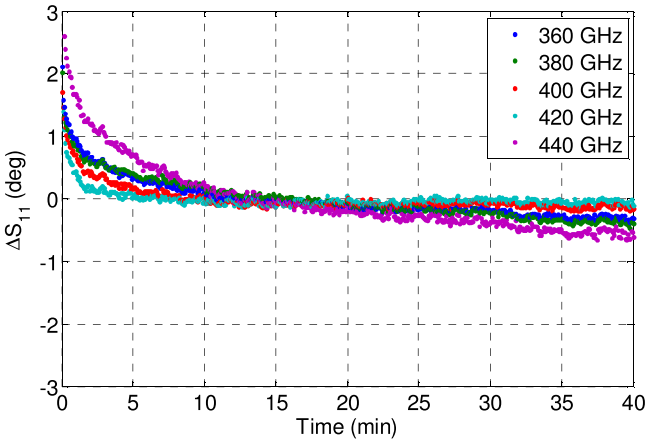

Fig. 11. Stability of the measured phase of S_{11} for a few frequencies.

achieved by utilizing a plano-convex lens and placing a horn antenna to locate the phase center in the focal point of the lens.

To measure reflection only from the sample under test, a two-step calibration procedure was used to remove unwanted reflections from objects in the setup (e.g., lens) and imperfections in measurement equipment. Initial calibration of the VNA with frequency extenders was made using the Line, Reflect, Line (LRL) method, with calibration standards provided by the manufacturer. In this case, the reference plane was achieved at the end of the waveguide port of the extender. Initial calibration minimizes residual errors from the second calibration stage.

The purpose of the second step of calibration was to eliminate the influence of unwanted reflections in the free space measurement system and to shift the measurement plane to the first face of the sample. The concept of the calibration of quasi-optical setup is described in detail in [13]. In this study, the Line, Reflect, Match (LRM) method was applied. To be able to realize this type of calibration, a sample holder was placed on a precision linear stage with 50 nm resolution. The stage was used only for Line measurement ensuring precision distance from reference plane to the reflective metal plate. Metal plate and electromagnetic absorber were used as calibration standards. Additionally, a time-domain gating was used to remove residual effects of unwanted reflections after LRM calibration.

After calibration, a sample of dielectric to be investigated was situated perpendicularly to the direction of wave propagation. The face of the sample was positioned at the determined measurement plane and only reflections from the tested sample were measured. Then, using (4) $\mathrm{CSWR}(f)$ was calculated.

There are several sources of measurement uncertainty in the presented method. Two main of them are related to residual calibration errors and reflection coefficient measurement errors. There are many papers (e.g., [7], [9]) concerning uncertainty analysis in similar setups. Different aspects were investigated, including measurement stability, repeatability of waveguide connections and focusing mismatch. To investigate the influence of these components on uncertainty in our measurement equipment, a standard Monte Carlo approach was utilized.

First, short-term stability (for 40 min) of S_{11} measurement for initially calibrated VNA was studied. It was done for all LRM calibration standards (used in the second tier of calibration procedure) and for two arbitrary chosen samples. Results were comparable for all measurements. Examples of amplitude and phase stability are presented in Figs. 10 and 11, respectively.

Monte Carlo simulation included LRM calibration and CSWR calculations assuming that normally distributed error of S_{11} measurement (after initial calibration) stated at 50% level of confidence is ± 0.03 for magnitude and $\pm 15°$ for phase. These numbers represent errors in initially corrected VNA measurements, imperfections of LRM standards, measurement stability, imperfect plane-wave approximation, and focusing mismatch. Monte Carlo analysis included four complex reflection coefficients in the frequency domain (related to three calibration standards and the sample under test).

In case of low-loss dielectrics, permittivity can be determined based on measured maxima of CSWR function. This approach enables fast and easy characterization of dielectric samples under test. However, this approach is not accurate. If permittivity

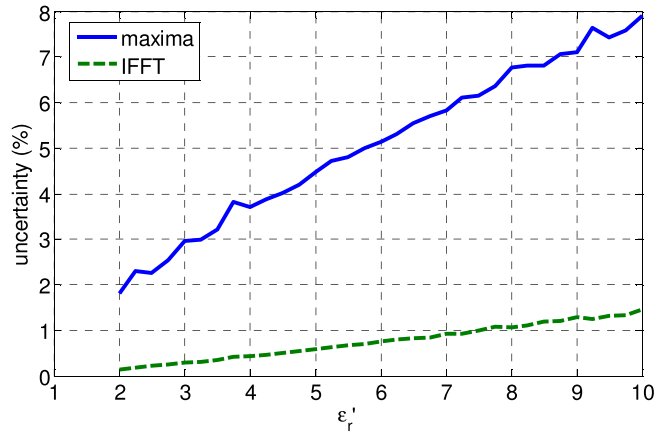

Fig. 12. Uncertainty of permittivity estimation for low-loss dielectrics obtained for two different methods.

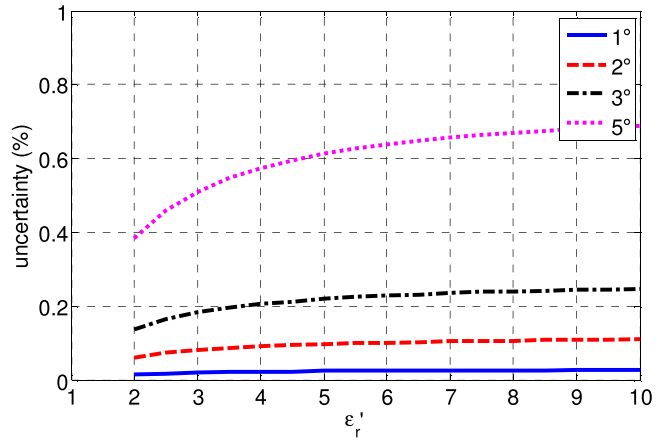

Fig. 13. Influence of sample tilt on permittivity uncertainty.

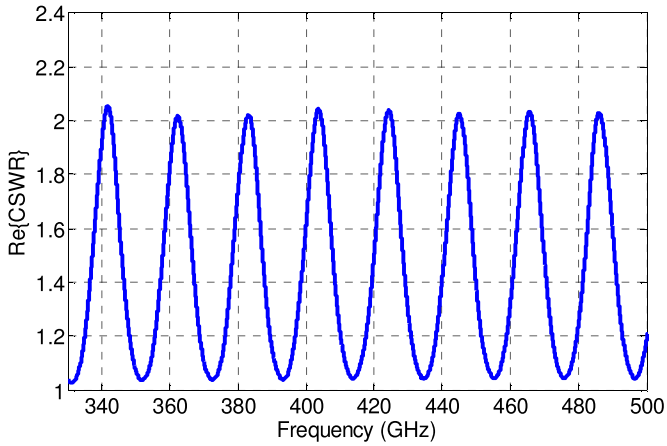

Fig. 14. Real part of CSWR distribution for PTFE sample.

TABLE I
MEASUREMENT RESULTS FOR PTFE SAMPLE

Frequency (GHz)	Relative Permittivity	
	This paper	Previously published [16]
341.9	2.06 ± 0.05	2.06
362.3	2.02 ± 0.04	2.06
383.2	2.02 ± 0.04	2.06
403.8	2.04 ± 0.05	2.055
424.3	2.04 ± 0.05	2.055
445.2	2.03 ± 0.04	2.055
465.6	2.03 ± 0.04	2.06
486.1	2.03 ± 0.04	2.05
325–500	Average permittivity $= 2.04 \pm 0.01$	

of a given dielectric has to be known more precisely, the average value of permittivity can be determined based on the Inverse Fourier Transform of $\mathrm{CSWR}(f)$ and (14) and (15). Comparison of uncertainty obtained using Monte Carlo simulations for these two concepts are presented in Fig. 12.

Uncertainty of loss tangent measurement is related mainly to errors in measuring of the phase of CSWR distribution. It has significant influence on low-loss dielectrics, for which average phase of $\mathrm{CSWR}(f)$ is relatively low (see Fig. 6).

Additional sources of uncertainty come from inappropriate placement of the sample under test and its irregular surface. In order to minimize unfavorable effects, the sample should have two flat and parallel faces. Moreover, it should be homogenous and sufficiently big to neglect diffraction on its edges. For samples used in experiments described in the next paragraph, all of these can be neglected. Only the influence of sample tilt was investigated. Fig. 13 presents uncertainty of permittivity measurements for lossless dielectrics with respect to sample tilt. We assumed that in the case of our measurements, tilt of the sample was not greater than $\pm 2°$.

It should be also emphasized that thickness of the sample is not used for calculating permittivity. However, the thicker the sample, the more maxima of CSWR distribution are measured, thus permittivity can be better approximated in the given frequency range. Another problem is related to frequency resolution and determination of $\mathrm{CSWR}(f)$ values at the given maxima; however, thanks to large number of frequency points in this study, maximum values can be accurately determined.

IV. Experimental Results

For verification of the proposed method, some experiments with low-loss as well as lossy dielectrics were conducted.

A. Low-Loss Dielectrics

The first tested dielectric sample was 5.05 mm thick and was made of polytetrafluoroethylene (PTFE). Measurement was performed in the $330-500$ GHz band. The real part of $\mathrm{CSWR}(f)$ distribution after calibration is shown in Fig. 14.

The real part of the permittivity can be directly read for each CSWR maximum. Measurement results are shown in Table I. Uncertainty of measurement for this approach is approximately $\pm 2\%$. Average permittivity in the 325–500 GHz frequency range calculated from the Inverse Fourier transform using (14) is more accurate (approximately $\pm 0.5\%$) and is also presented in Table I. Average phase of measured CSWR

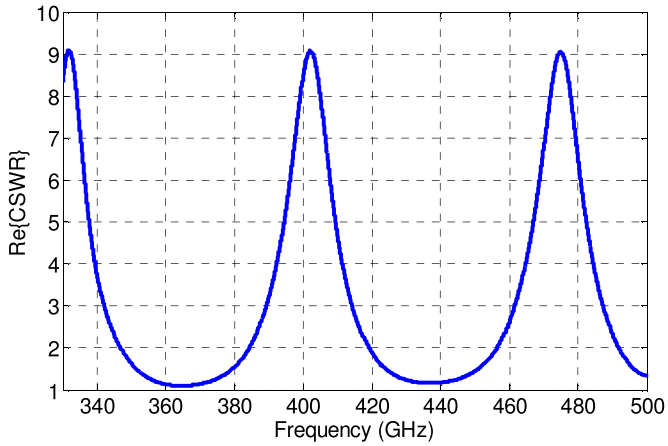

Fig. 15. Real part of CSWR distribution for alumina sample.

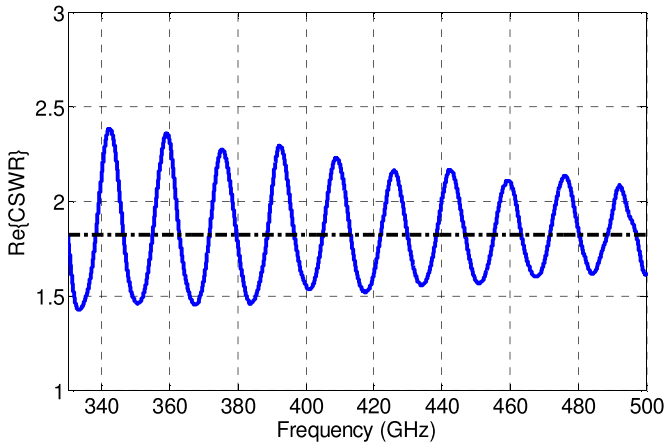

Fig. 16. Real part of CSWR distribution for lossy LTCC sample.

TABLE II
MEASUREMENT RESULTS FOR ALUMINA SAMPLE

Frequency (GHz)	Relative Permittivity	
	This paper	Previously published [17]
332.1	9.11 ± 0.64	9.36
402.4	9.08 ± 0.63	9.36
475.1	9.06 ± 0.63	
325–500	Average permittivity $= 9.09 \pm 0.15$	

function is close to zero, thus one can find that loss tangent is lower than 0.001.

The second investigated low-loss material was alumina (Al_2O_3). The sample had 0.68 mm in thickness, resulting in only three maxima of CSWR distribution in the given frequency band. The result is shown in Fig. 15 and in Table II. Average permittivity in the given frequency range is also presented. Loss tangent is lower than 0.01 due to the fact that average phase of $\mathrm{CSWR}(f)$ is close to zero.

B. Lossy Dielectrics

In Figs. 16 and 17, results for 4.94-mm-thick sample made of laboratory-developed low-temperature cofired ceramics (LTCC) material are presented. As expected, the higher the frequency, the lower the maxima of CSWR distribution.

Using (14) and (15), the real part of permittivity and loss tangent of tested material were determined. Average real part of permittivity is equal to 3.31 ± 0.02 and average loss tangent is equal to 0.015 ± 0.003.

Another lossy dielectric that was investigated was PMMA—poly(methyl methacrylate). The sample under test was 25 mm thick. In conjunction with relatively high losses it results that obtained CSWR function has no ripples (see Figs. 18 and 19), therefore complex permittivity can be easily calculated from (7) and (8).

The real part of permittivity is approximately 2.59 ± 0.02 in the investigated frequency band and it is comparable with previously published results (2.56–2.58) [18]. Average phase of CSWR is equal to 0.72° which translates to loss tangent of 0.025 ± 0.003.

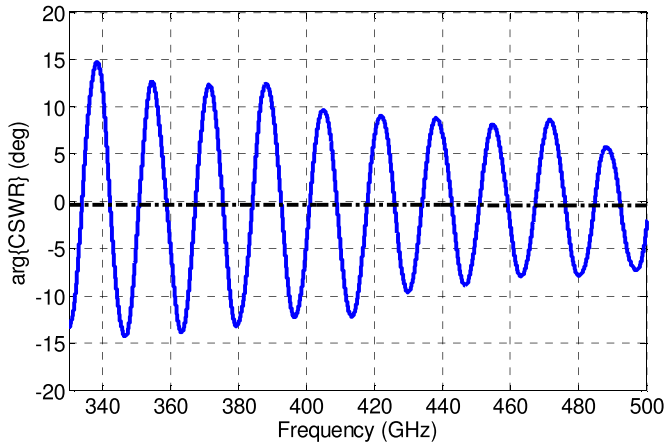

Fig. 17. Phase of CSWR distribution for lossy LTCC sample.

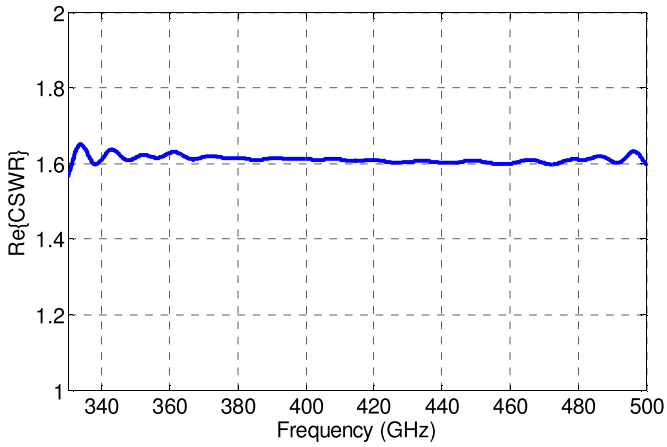

Fig. 18. Real part of CSWR distribution for lossy PMMA sample.

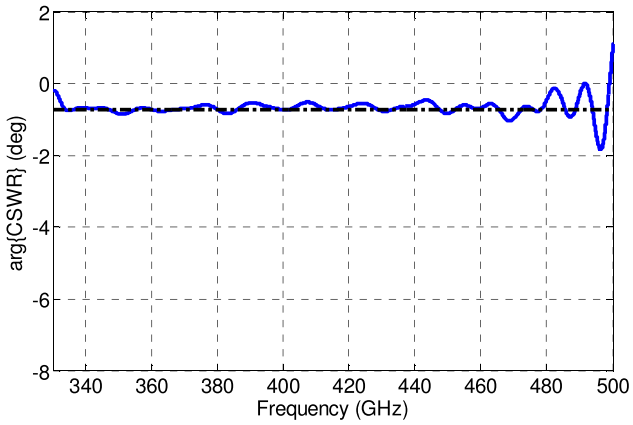

Fig. 19. Phase of CSWR distribution for lossy PMMA sample.

V. Conclusion

In this paper a new method for characterization of dielectrics at sub-THz frequencies has been presented. The method is based on capabilities of modern measurement instrumentation. A few different materials were tested to verify the proposed measurement procedure. Results prove that this method can be used for characterization of both lossless and lossy dielectric samples with sufficient but not precisely determined thickness. In the case of some types of materials (especially dispersive dielectrics) sufficiently thick sample has to be tested. It can be a limitation if such a sample is not available. One of the most important advantages of this newly developed method is that it requires only the complex reflection coefficient for permittivity characterization. Moreover, precision of the proposed method is comparable to other quasi-optical methods presented in the literature. In addition, since the method does not need information about thickness of dielectric samples, it opens up new measurement possibilities allowing remote characterization.

References

[1] J. Krupka, "Frequency domain complex permittivity measurements at microwave frequencies," *Meas. Sci. Technol.*, vol. 17, no. 6, pp. 55–70, 2006.

[2] L. F. Chen, C. K. Ong, C. P. Neo, V. V. Varadan, and V. K. Varadan, *Microwave Electronics: Measurement and Materials Characterization*. Chichester, U.K.: Wiley, 2004.

[3] Y. Kobayashi and S. Tanaka, "Resonant modes of a dielectric rod resonator short-circuited at both ends by parallel conducting plates," *IEEE Trans. Microw. Theory Techn.*, vol. 28, no. 10, pp. 1077–1085, Oct. 1980.

[4] A. Kaczkowski and A. Milewski, "High-Accuracy wide-range measurement method for determination of complex permittivity in reentrant cavity: Part A—Theoretical analysis of the method," *IEEE Trans. Microw. Theory Techn.*, vol. 28, no. 3, pp. 225–228, Mar. 1980.

[5] J. Krupka, D. Cros, M. Aubourg, and P. Guillon, "Study of whispering gallery modes in anisotropic single-crystal dielectric resonators," *IEEE Trans. Microw. Theory Techn.*, vol. 42, no. 1, pp. 56–61, Jan. 1994.

[6] N. A. Andrushchak, Y. V. Bobitskii, T. V. Maksymyuk, O. I. Syrotynsky, A. S. Andrushchak, and I. D. Karbovnyk, "A new method for refractive index measurement of isotropic and anisotropic materials in millimeter and submillimeter wave range," in *Proc. 18th Int. Conf. Microw. Radar Wireless Commun.,* Vilnius, Lithuania, 2010, pp. 1–3.

[7] D. K. Ghodgaonkar, V. V. Varadan, and V. K. Varadan, "Free-space measurement of complex permittivity and complex permeability of magnetic materials at microwave frequencies," *IEEE Tran. Instrum. Meas.*, vol. 39, no. 2, pp. 387–394, Apr. 1990.

[8] V. V. Varadan, R. D. Hollinger, D. K. Ghodgaonkar, and V. K. Varadan, "Free-space, broadband measurements of high-temperature, complex dielectric properties at microwave frequencies," *IEEE Trans. Instrum. Meas.*, vol. 40, no. 5, pp. 842–846, Oct. 1991.

[9] A. Kazemipour *et al.*, "Design and calibration of a compact quasi-optical system for material characterization in millimeter/submillimeter wave domain," *IEEE Trans. Instrum. Meas.*, vol. 64, no. 6, pp. 1438–1445, Jun. 2015.

[10] M. Naftaly, "Metrology issues and solutions in THz time-domain spectroscopy: Noise, errors, calibration," *IEEE Sensors J.*, vol. 13, no. 1, pp. 8–17, Jan. 2013.

[11] N. A. Andrushchak, I. D. Karbovnyk, K. Godziszewski, Y. Yashchyshyn, M. V. Lobur, and A. S. Andrushchak, "New interference technique for determination of low loss material permittivity in the extremely high frequency range," *IEEE Trans. Instrum. Meas.*, vol. 64, no. 11, pp. 3005–3012, Nov. 2015.

[12] K. Godziszewski and Y. Yashchyshyn, "Investigation of influence of measurement conditions on accuracy of material characterization in sub-THz frequency range," in *Proc. 21st Int. Conf. Microw., Radar Wireless Commun.,* Krakow, Poland, 2016, pp. 1–4.

[13] D. Bourreau, A. Peden, and S. Le Maguer, "A quasi-optical free-space measurement setup without time-domain gating for material characterization in the W-band," *IEEE Trans. Instrum. Meas.*, vol. 55, no. 6, pp. 2022–2028, Dec. 2006.

[14] Keysigtht Technologies, "Keysight 2-Port and 4-Port PNA-X Network Analyzer," Nov. 7, 2016. [Online]. Available: http://literature.cdn.keysight.com/litweb/pdf/N5245-90008.pdf. Accessed on: Nov. 18, 2016.

[15] Virginia Diodes, Inc. "VNA Extension Modules. Operational Manual," Apr. 26, 2017. [Online]. Available: http://www.vadiodes.com/images/Products/VNA/VDI-707.1VNAxProductManual.pdf. Accessed on: Jun. 30, 2017.

[16] T. Chang, X. Zhang, C. Yang, Z. Sun, and H. Cui, "Measurement of complex terahertz dielectric properties of polymers using an improved free-space technique," *Meas. Sci. Technol.*, vol. 28, no. 4, pp. 1–8, Feb. 2017.

[17] M. Afsar, "Precision millimeter-wave dielectric measurements of birefringent crystalline sapphire and ceramic alumina," *IEEE Trans. Instrum. Meas.*, vol. 36, no. 2, pp. 554–559, Jun. 1987.

[18] M. Naftaly and R. Miles, "Terahertz time-domain spectroscopy for material characterization," *Proc. IEEE*, vol. 95, no. 8, pp. 1658–1665, Aug. 2007.

Yevhen Yashchyshyn (M'96–SM'09) received the M.Sc. degree from Lviv Polytechnic National University, Lviv Oblast, Ukraine, in 1979, the Ph.D. degree from Moscow Institute of Electronics and Mathematics (MIEM), Moscow, Russia, in 1986, and the D.Sc. (Habilitation) degree from the Warsaw University of Technology (WUT), Warsaw, Poland, in 2006.

Since 1999, he has been with the Institute of Radioelectronics (IR), WUT, where he became the Head of the Antenna Laboratory in 2002. From 2009 to 2016, he was the Head of the Radiocommunication Division, WUT. Since 2016, he has been the Deputy Director for Research of IRiTM, WUT. He has authored over 200 technical papers, authored or coauthored 4 books, and holds a few patents. His current research interests include antenna theory and techniques, smart beamforming, reconfigurable antennas, radio over fiber techniques, and materials characterization, including ferroelectric ceramic-polymers composites investigation up to subterahertz frequency.

Prof. Yashchyshyn was the recipient of the First Prize of EuMA at the 11th European Microwave Week for his outstanding research and new concept of the reconfigurable antenna, Amsterdam, The Netherlands, 2008.

Konrad Godziszewski (S'12–M'17) was born in Warsaw, Poland, in 1986. He received the M.Sc. degree in electronics and telecommunications engineering in 2011 from the Warsaw University of Technology (WUT), Warsaw, Poland, where he is currently working toward Ph.D. degree.

He joined the Institute of Radioelectronics, WUT, in 2013. He has authored or coauthored over 30 technical papers. His current research interests include material characterization in subterahertz frequency range, ferroelectric materials, and antenna techniques.